IMECE2011-64498

RHEOLOGICAL STUDY ON MULTIPLE FIBER SUSPENSIONS FOR FIBER REINFORCED COMPOSITE MATERIALS PROCESSING

Dongdong Zhang
Department of Mechanical & Aerospace Engineering
University of Missouri, Columbia, MO, USA
dz25c@mail.missouri.edu

Douglas E. Smith
Department of Mechanical & Aerospace Engineering
University of Missouri, Columbia, MO, USA
SmithDoug@missouri.edu

David A. Jack
Department of Mechanical Engineering
Baylor University, Waco, Texas, USA
David_Jack@baylor.edu

Stephen Montgomery-Smith
Department of Mathematics
University of Missouri, Columbia, MO, USA
stephen@missouri.edu

ABSTRACT

This paper studies the rheological properties of a semi-dilute fiber suspension for short fiber reinforced composite materials processing. For industrial applications, the volume fraction of short fibers could be large for semi-dilute and concentrated fiber suspensions. Therefore, fiber-fiber interactions consisting of hydrodynamic interactions and direct mechanical contacts could affect fiber orientations and thus the rate of fiber alignment in the manufacturing processing. In this paper, we study the semi-dilute fiber suspensions, i.e. the gap between fibers becomes closer, and hydrodynamic interactions becomes stronger, but the physical/mechanical contacts are still rare. We develop a three-dimensional finite element approach for simulating the motions of multiple fibers in low-Reynolds-number flows typical of polymer melt flow. We extend our earlier single fiber model to consider hydrodynamic interactions between fibers. This approach computes the hydrodynamic forces and torques on fibers by solving governing equations of motion in fluid. The hydrodynamic forces and torques result from two scenarios: gross fluid motion and hydrodynamic interactions from other fibers. Our approach seeks fibers' velocities that zero the hydrodynamic torques and forces acting on the fibers by the surrounding fluid. Fiber motions are then computed using a Runge-Kutta approach to update fiber positions and orientations as a function of time. This method is quite general and allows for solving multiple fiber suspensions in complex fluids. Examples with fibers having various starting positions and orientations are considered and compared with Jeffery's single fiber solution (1922). Meanwhile, we study the effect of the presence of a bounded wall on fiber motions, which is ignored in Jeffery's original work. The possible reasons why fiber motions observed in experiments align slower than those predicted by Jeffery's theory are discussed in this paper.

INTRODUCTION

Fiber reinforced polymer composite materials, well-known for high strength-to-weight ratio, are widely used in various industries such as aerospace and automotive fields. The mechanical, electrical and thermal properties of short fiber reinforced composite materials could be largely improved by adding up to 50% carbon or glass micro-size fibers into the polymer matrix. Therefore, the physical/rheological properties of fiber reinforced composite systems are tremendously dependent on fiber orientations within the polymer matrix which is determined during the manufacturing process. The orientation state of fibers is often computed based on the model first

proposed by Jeffery [1], who studied a single ellipsoidal fiber moving in a Newtonian, incompressible, homogeneous flow. While Jeffery's model has received wide acceptance in the mold filling community, experiments have shown that fiber alignment occurs more slowly than that predicted by Jeffery-based models ([2], [3]), which may result from such limiting assumption of having no fiber-fiber interactions in Jeffery's original work. Likewise, Stover *et al.* [4] experimentally measured fiber motions in semi-dilute suspensions, and found that fiber orientations are different from those in dilute suspensions. Additionally, the presence of a bounded wall could also change the rheological behavior of polymer matrix. Therefore, this paper studies the semi-dilute fiber suspensions and the effect of a bounded wall on fiber orientations. The followings as related to fiber orientations in composite molding processes are studied:

- A methodology is proposed to numerically solve multiple fiber motions in semi-dilute suspensions. This approach combines a finite element method, a Newton-Raphson iteration method and a Runge-Kutta method.

- Hydrodynamic interactions between fibers are modeled. With the presence of multiple fibers, the motion of one fiber affects its surrounding fluid which influences the dynamics of other fibers, and vice versa.

- Fiber orientations in a bounded shear flow are studied. The changes of fiber motions and time periods of rotation with the presence of a bounded wall are observed in our simulation.

The remainder of this paper is organized as follows: Section 1 introduces Jeffery's theory and related background information. Section 2 elucidates the methodology, including the finite element method, the Newton-Raphson iteration approach and the Runge-Kutta method. Section 3 presents the effect of a bounded wall on fiber motions. Section 4 gives some examples to validate the proposed methodology. Conclusions and future work are presented in section 5.
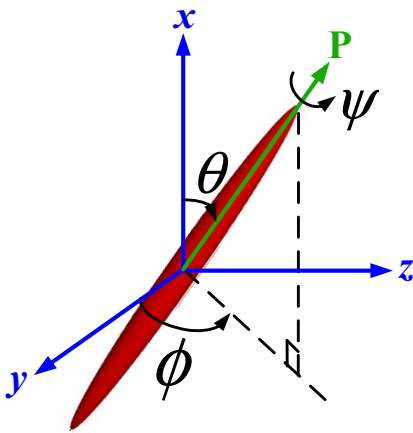

FIGURE 1. Definition of a single ellipsoidal fiber orientation

1 BACKGROUND AND LITERATURE REVIEW

Jeffery [1] first derived the equations of motion for the dynamics of a single ellipsoidal fiber suspended in a simple shear flow. In Jeffery's theory, fiber orientations are defined by three angles (ϕ, θ, ψ) in terms of the global coordinate system *xyz*, as shown in Fig.1. The angles ϕ and θ are used to define the unit direction of the primary axis, often defined as **P**, and ψ represents the rotation along **P**. Jeffery applied the zero-torque condition on fiber and derived the differential equations, with the solutions of ϕ, θ, ψ shown as follows.

$$\phi(t) = \tan^{-1}\left(r_e \tan\frac{\dot{\gamma}\,t}{r_e + 1/r_e} \right) \quad (1)$$

$$\theta(t) = \tan^{-1}\frac{C\,r_e}{\sqrt{r_e^2\cos^2\phi + \sin^2\phi}} \quad (2)$$

$$\psi(t) = \int_0^t \left(\frac{\dot{\gamma}}{2} - \dot{\phi} \right)\cos\theta\,dt \quad (3)$$

where $\dot{\gamma}$ is the shear rate of the simple shear flow, r_e is the ratio of long-axis to short axis of the ellipsoid, often referred to as geometric aspect ratio. For other shapes of fibers, such as cylindrical fibers, the equivalent aspect ratio (r_e^*) should be used to quantify fiber motions ([5]), and those of cylinders and bead-chain fibers were produced by Zhang, *et al.* [6]. The constant C is determined by the initial fiber orientation (ϕ_0, θ_0) and can be calculated as $C = \tan\theta_0\sqrt{\cos^2\phi_0 + \sin^2\phi_0/r_e^2}$.

Jeffery's theory was later extended to a single fiber suspension in other homogeneous flows ([7], [8]). Two important simplifications are made in Jeffery's theory: 1) Fiber-fiber interactions are totally ignored. However, in the composite molding process, the volume fraction of fibers may be high; 2) Fiber exists in an unbounded fluid domain, i.e., the ratio of fiber dimension versus the size of fluid domain goes to zero. However, in the manufacturing process, the outside wall (cavity) exists, which would change the rheological behavior of the polymer matrix. Therefore, the existence of other fibers or a bounded wall could affect fiber orientations, which has attracted many attentions in the rheological academic community.

In terms of fiber-fiber interactions, there are basically three approaches:

1) Continuum mechanics: Batchelor [9] and Dinh [10] modified the stress constitutive equation to take into account the effect of fiber-fiber interactions on the total stress, and thus the fiber motions. But no constitutive equation is available in a closed form.

2) Statistical mechanics: From the statistical perspective, the orientation distribution function was proposed to describe the probability of fiber orientations pointing in certain direction **P**, and a diffusion term is added to account for
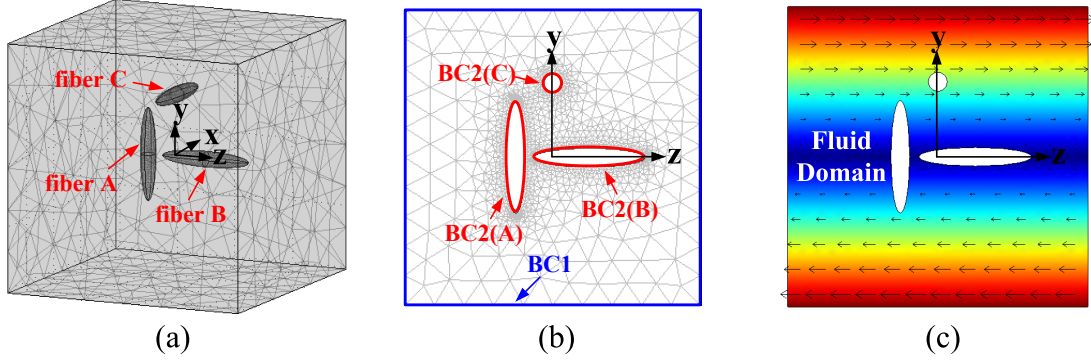
FIGURE 2. Finite element model of multiple fiber suspensions with specified boundary conditions

fiber-fiber interactions [11]. The orientation averaging using diffusion-added orientation distribution function yields the orientation tensor approach [7]. Multiple closure approximations are proposed to address the closure issue of orientation tensor approach [12].

3) Physical modeling: The inter-fiber hydrodynamic interactions are approximated and simulated using different methods. Mackaplow [13] and Rahnama [14] used slender-body theory to describe the long-range hydrodynamic interactions. Yamane [15] considered the short-range interactions between rod-like fibers by using lubrication approximation. Fan [16] applied slender body theory to approximate long-range hydrodynamic interactions and used lubrication approximation to calculate short-range interactions between fibers. Claeys [17] treated the hydrodynamic interactions from multiple other fibers as a single force and toque on the fiber.

There are not many studies on fiber motions in a bounded flow. Junk [8] theoretically analyzed the effect of a bounded wall around the fiber, and pointed out that Jeffery's result represents the leading order solution of a singularly perturbed flow problem. Stover [18] experimentally studied fiber motions near a bounded wall, and found that particles aligned with the flow direction and less than a particle half-length from a wall remain indefinitely. Jayageeth [19] simulated the short fiber suspension in a bounded shear flow using stokesian dynamics simulation, and indicated that the time periods of rotations increase as the fiber moves closer to the wall.

In this paper, we focus on the study of hydrodynamic interactions between multiple fibers and the disturbance effects of a bounded wall on fiber motions. The finite element method is applied to calculate the forces and torques exerted on each fiber. The force and torque distribution around the fiber will be distinct with the presence of other fibers or a bounded wall in close proximity.

2 METHODOLOGY

In our methodology, we use a finite element model to represent the fluid domain between multiple fibers and the outside bounded wall (cavity). Velocity and pressure distribution in fluid domain are calculated using a finite element method with the velocity boundaries specified on fiber surfaces and the bounded wall. Our method searches fibers' linear and angular velocities, which zero the net forces and torques exerted by the surrounding fluid on fibers. The forces and torques come from two scenarios: gross moving fluid and hydrodynamic interactions from other fibers. This method solves both long-range and short-range interactions (lubrication effect) simultaneously. Our methodology is described as follows:

2.1 Finite element model

The fluid domain is modeled as tetrahedral meshes, as shown in Fig.2(a). The velocity boundary conditions are specified on fiber surfaces and the outside wall, as shown in Fig.2(b), in which BC2(A) refers to the velocity boundary on the surface of fiber A. The governing equations in fluid are:

$$\nabla \cdot \mathbf{U} = 0 \tag{4}$$
$$\mu \nabla^2 \mathbf{U} = \nabla p \tag{5}$$

where μ is the viscosity of bulk flow, $\mathbf{U}$ is the velocity vector in fluid, and p is the pressure distribution in fluid. The boundary conditions used for solving velocity and pressure distribution are:
(BC1) On the bounded wall (cavity):

$$\mathbf{U}_{\text{BC1}} = \mathbf{U}_0 \tag{6}$$

(BC2) On the fiber surface (e.g., for fiber A):

$$\mathbf{U}_{\text{BC2(A)}} = \mathbf{U}_c^{A} + \boldsymbol{\omega}^{A} \times \mathbf{r} \tag{7}$$

3

where $\mathbf{U}_0$ is the undisturbed shear flow, $\mathbf{r}$ is the displacement vector of point on fiber surface, $\mathbf{U}_c^A = [\dot{x}_c, \dot{y}_c, \dot{z}_c]$ is the translation velocity of fiber A's centroid, and $\boldsymbol{\omega}^A = [\omega_x^A, \omega_y^A, \omega_z^A]^T$ is the angular velocity of fiber A with respect to the global coordinate system xyz, defined as

$$\boldsymbol{\omega}^A = \begin{bmatrix} \omega_x^A \\ \omega_y^A \\ \omega_z^A \end{bmatrix} = \begin{bmatrix} \dot{\phi} + \dot{\psi}\cos\theta \\ -\dot{\theta}\sin\phi + \dot{\psi}\sin\theta\cos\phi \\ \dot{\theta}\cos\phi + \dot{\psi}\sin\theta\sin\phi \end{bmatrix} \quad (8)$$

Therefore, the boundary condition specified on the surface of fiber A is defined by the translation velocities of fiber A's centroid and its angular velocities. In a similar manner, for fibers B, C and so on, the velocity boundary conditions BC2(B), BC2(C), *etc.* can be specified. Provided that all fibers' linear and angular velocities are known, the governing equations (cf. Eqs.(4) and (5)) could be solved using the finite element method, and in turn the velocity and pressure distribution in bulk fluid can be obtained.

2.2 Hydrodynamic force/torque

With the calculated velocity distribution $\mathbf{U}$ and pressure distribution p in fluid, force and torque vector exerted on fiber A can be calculated as

$$\boldsymbol{\sigma} = -p\boldsymbol{\delta} + \mu[\nabla\mathbf{U} + (\nabla\mathbf{U})^T] \quad (9)$$

$$\mathbf{F}^A = \int \{\boldsymbol{\sigma}\cdot\mathbf{n}\}dS \quad (10)$$

$$\mathbf{T}^A = \int \{\mathbf{r}\times(\boldsymbol{\sigma}\cdot\mathbf{n})\}dS \quad (11)$$

where $\boldsymbol{\sigma}$ is the total stress in fluid, $\boldsymbol{\delta}$ is the Kronecker detla, dS is the surface integral, $\mathbf{n}$ is the unit normal vector on fiber surface and $\mathbf{r}$ is same as that in Eq.(7). $\mathbf{F}^A$ and $\mathbf{T}^A$ are, respectively, net force and net torque on fiber A.

Likewise, forces and torques exerted on fibers B, C, *etc.* can be obtained. In a simple shear flow, a single fiber performs a periodic tumbling motion within the moving fluid, described as "Jeffery's oribt". When multiple fibers suspend in the fluid, the hydrodynamic interactions between fibers come into play. Specifically, the motion of one fiber will affect its surrounding fluid, and in turn influence the motions of other fibers, and vice versa. Therefore, the forces and torques on fiber A depend on not only fiber A's velocities, but also the motions of other fibers. The force and torque vector on fiber A can be represented as

$$\mathbf{F}^A = \mathbf{F}^A(\dot{x}_c^A, \dot{y}_c^A, \dot{z}_c^A, \dot{\phi}^A, \dot{\theta}^A, \dot{\psi}^A, \dot{x}_c^B, \dot{y}_c^B, \dot{z}_c^B, \dot{\phi}^B, \dot{\theta}^B, \dot{\psi}^B, \cdots) \quad (12)$$

$$\mathbf{T}^A = \mathbf{T}^A(\dot{x}_c^A, \dot{y}_c^A, \dot{z}_c^A, \dot{\phi}^A, \dot{\theta}^A, \dot{\psi}^A, \dot{x}_c^B, \dot{y}_c^B, \dot{z}_c^B, \dot{\phi}^B, \dot{\theta}^B, \dot{\psi}^B, \cdots) \quad (13)$$

For fiber motions, the mass and mass moment of inertia of small suspended fibers could be neglected, so the resultant forces and torques on all fibers are always zero at each time instant. Therefore, the linear and angular velocities of all fibers can be calculated by solving the following system of equations.

$$\begin{cases} \mathbf{F}^A(\dot{x}_c^A, \dot{y}_c^A, \dot{z}_c^A, \dot{\phi}^A, \dot{\theta}^A, \dot{\psi}^A, \dot{x}_c^B, \dot{y}_c^B, \dot{z}_c^B, \dot{\phi}^B, \dot{\theta}^B, \dot{\psi}^B, \cdots) = \mathbf{0} \\ \mathbf{T}^A(\dot{x}_c^A, \dot{y}_c^A, \dot{z}_c^A, \dot{\phi}^A, \dot{\theta}^A, \dot{\psi}^A, \dot{x}_c^B, \dot{y}_c^B, \dot{z}_c^B, \dot{\phi}^B, \dot{\theta}^B, \dot{\psi}^B, \cdots) = \mathbf{0} \\ \mathbf{F}^B(\dot{x}_c^A, \dot{y}_c^A, \dot{z}_c^A, \dot{\phi}^A, \dot{\theta}^A, \dot{\psi}^A, \dot{x}_c^B, \dot{y}_c^B, \dot{z}_c^B, \dot{\phi}^B, \dot{\theta}^B, \dot{\psi}^B, \cdots) = \mathbf{0} \\ \mathbf{T}^B(\dot{x}_c^A, \dot{y}_c^A, \dot{z}_c^A, \dot{\phi}^A, \dot{\theta}^A, \dot{\psi}^A, \dot{x}_c^B, \dot{y}_c^B, \dot{z}_c^B, \dot{\phi}^B, \dot{\theta}^B, \dot{\psi}^B, \cdots) = \mathbf{0} \\ \quad\cdots\cdots\cdots\cdots \end{cases}$$
$$(14)$$

If there are two fibers (A and B) in the fluid, there are twelve unknowns and twelve force/torque equilibrium equations ($\mathbf{F} = [F_x, F_y, F_z]$ and $\mathbf{T} = [T_x, T_y, T_z]$). Therefore, the velocities of fibers at each time moment can be solved using a Newton-Raphson iteration algorithm.

2.3 Update fiber orientations/positions

At each time step t_i, provided that fiber positions and orientations are given, the linear velocities of fiber centroid ($\dot{x}_c, \dot{y}_c, \dot{z}_c$) and angular velocities (defined by $\dot{\phi}, \dot{\theta}, \dot{\psi}$) are obtained by solving Eq.(14) to give $\dot{\mathbf{y}}_i = \mathbf{f}(t_i, \mathbf{y}_i)$, where $\mathbf{y} = [x_c^A, y_c^A, z_c^A, \phi^A, \theta^A, \psi^A, x_c^B, y_c^B, z_c^B, \phi^B, \theta^B, \psi^B, \cdots]$. With the specified time interval Δt, we apply the 4th-order Runge-Kutta algorithm to update fiber orientations (ϕ, θ, ψ) and centroid positions (x_c, y_c, z_c) in the next time time step t_{i+1} ($= t_i + \triangle t$). The algorithm is shown as follows:

$$\mathbf{y}_{i+1} = \mathbf{y}_i + \frac{1}{6}\Delta t(\mathbf{k}_1 + 2\mathbf{k}_2 + 2\mathbf{k}_3 + \mathbf{k}_4) \quad (15)$$

where

$$\mathbf{k}_1 = \mathbf{f}(t_i, \mathbf{y}_i)$$
$$\mathbf{k}_2 = \mathbf{f}(t_i + 0.5\Delta t, \mathbf{y}_i + 0.5\mathbf{k}_1\Delta t)$$
$$\mathbf{k}_3 = \mathbf{f}(t_i + 0.5\Delta t, \mathbf{y}_i + 0.5\mathbf{k}_2\Delta t)$$
$$\mathbf{k}_4 = \mathbf{f}(t_i + \Delta t, \mathbf{y}_i + \mathbf{k}_3\Delta t)$$

3 EFFECT OF BOUNDED WALL

Experiments have shown that the fiber motion is observed to have a longer period than that predicted by Jeffery. One possible explanation is the existence of a bounded wall (cavity) in experiments, while the fluid domain is assumed to be infinite in Jeffery's theory. The dimensionless parameter to quantify the wall effect is

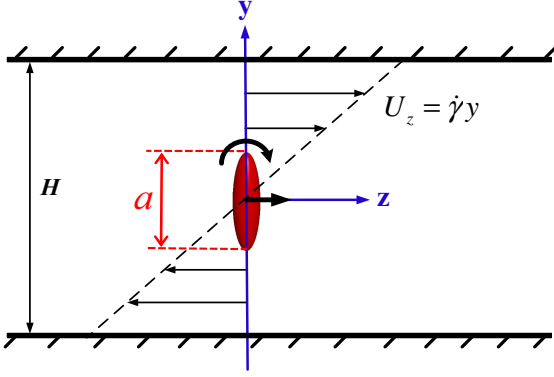$$\varepsilon = \frac{a}{H} \quad (16)$$

FIGURE 3. Definition of wall effect: the ratio of fiber dimension to the gap of two parallel wall

where a is the long axis of an ellipsoidal fiber, or the length of a cylindrical fiber. H is the distance between the bounded wall, shown in Fig.3. In Jeffery's theory, the fiber exists in an unbounded fluid, i.e., $H = \infty$ and $\varepsilon = 0$. However, the existence of a bounded wall would change the velocity and pressure distribution in bulk fluid. This has been approved in a similar problem that a creeping uniform flow passes a fixed sphere in an unbounded domain ([20], [21]), seen in Fig.4. The exact solution to that problem ([21]) is

$$\mathbf{U} = \mathbf{U}_\infty - \frac{3a}{8}\left[\frac{\mathbf{U}_\infty}{r} + \frac{\mathbf{r}\,\mathbf{U}_\infty \cdot \mathbf{r}}{r^3}\right] - \frac{a^3}{32}\left[\frac{\mathbf{U}_\infty}{r^3} - 3\frac{\mathbf{r}\,\mathbf{U}_\infty \cdot \mathbf{r}}{r^5}\right] \quad (17)$$

where a is the diameter of the spherical fiber, $\mathbf{U}_\infty$ is the undisturbed uniform fluid, $\mathbf{r}$ is the displacement vector in fluid, and r is the magnitude of displacement vector. From the exact solution of velocity distribution, we can see that at the position where $r = 5a$, i.e. $\varepsilon = a/r = 0.2$, U differs from U_∞ by about 8%. That is to say, if $\mathbf{U}_\infty$ is specified at $r = 5a$, the velocity distribution will deviate from Eq.(17), and depend on how far away the wall is from the fiber.

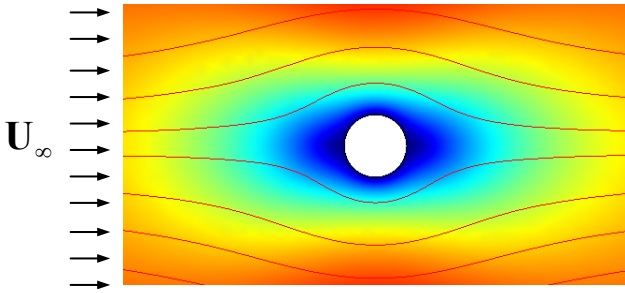In an analogous manner, for fiber suspensions, the presence

FIGURE 4. Uniform flow passes a fixed sphere in an unbounded fluid domain

of wall also change the velocity and pressure distributions, and in turn the fiber motions. In our methodology, we specify the undisturbed simple shear flow on the bounded wall, which has a finite distance from the fiber, so $\varepsilon \neq 0$. In our earlier work [6], we showed that when $\varepsilon \leq 0.025$, our results to solve a single fiber motion within a viscous fluid are in an excellent agreement with Jeffery's solution. In this paper, we study the effect of different $\varepsilon's$ on fiber orientations. We use a finite element method to simulate a single fiber motion in a bounded fluid domain with different dimensions. The results are shown in section 4.2.

4 EXAMPLES AND IMPLEMENTATIONS

In this section, some examples are presented to validate the proposed methodology. We use COMSOL to solve the governing equations (cf. Eqs.(4) and (5)) in fluid using a finite element method. Matlab is used to implement Newton-Raphson and Runge-Kutta algorithm.

4.1 Hydrodynamic interactions

The parameter to quantify the effect of hydrodynamic interactions is the ratio of fiber dimension to the distance between fiber centroids, defined as:

$$\zeta = \frac{a}{D} \quad (18)$$

where D is the distance between the centroids of two fibers, seen in Fig.5. When $D \gg a$, the long-range hydrodynamic interactions come into play, and when D is close to a, the short-range hydrodynamic interactions dominate. In this section, various examples with different distances between fiber centroids are presented. Fiber angles and positions are updated using a Runge-Kutta method, and compared with Jeffery's solution (cf. Eqs.(1-3)) in the work below.

Any axisymmetric fiber has the same rotation as that of the ellipsoidal fiber, but the equivalent aspect ratio r_e^* needs to be used instead of geometric aspect ratio r_e ([5, 6]). In this section, we study the hydrodynamic interactions between fibers with different shapes, including ellipsoidal and cylindrical fibers.
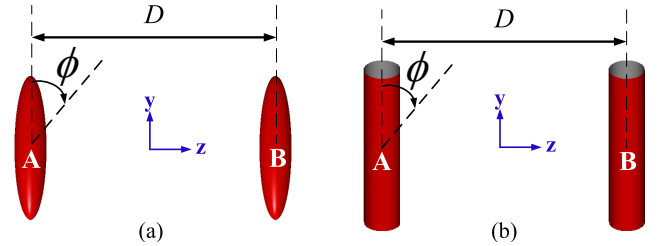

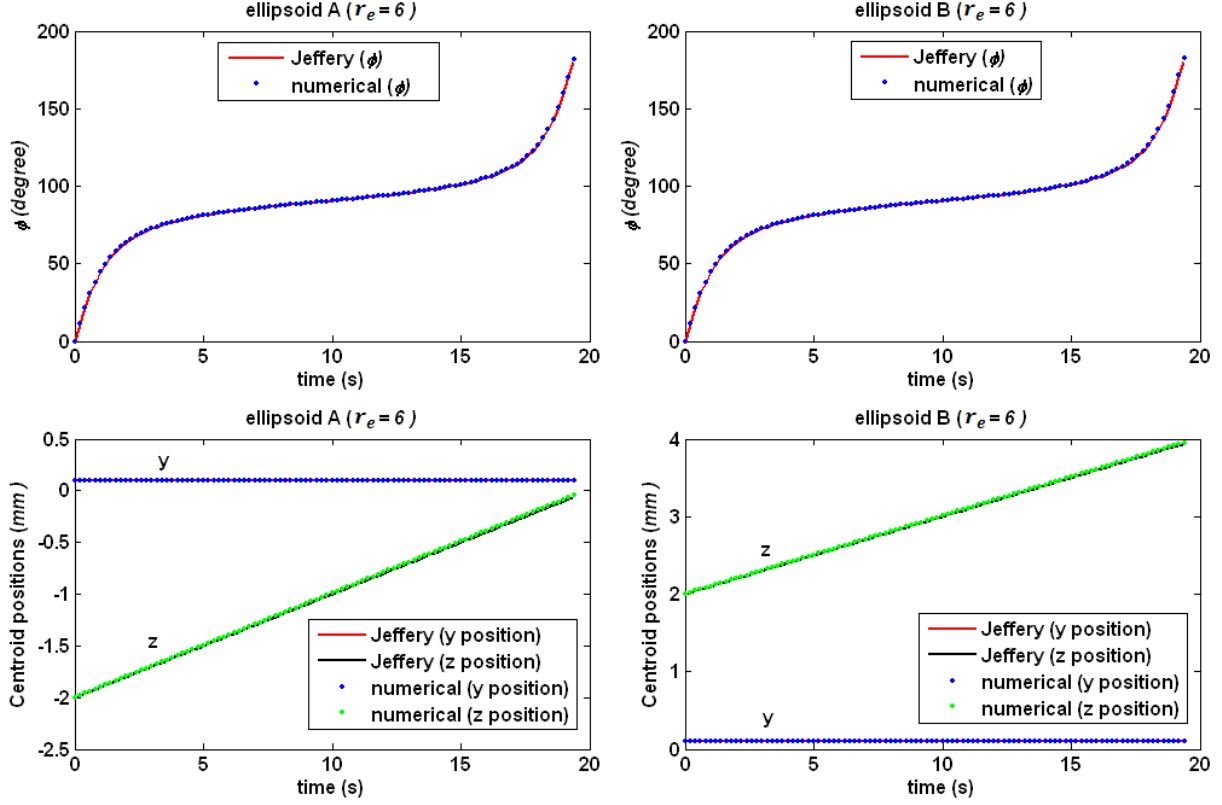**FIGURE 5**. Initial configurations of two fibers: (a) two ellipsoids; (b) two cylinders

FIGURE 6. Fiber positions and orientations in half period: two far-away ellipsoidal fibers ($\zeta = 0.075 \ll 1$)

4.1.1 Fibers are far away from each other

When two fibers are far away, i.e. $H \gg a$ and $\zeta \ll 1$, the hydrodynamic interactions, called long-range interactions, are trivial, which cannot visibly affect fiber motions. Here, we model two far-away ellipsoidal fibers, with the initial configuration shown in Fig.5(a) and the simulation parameters are tabulated in Table 1. The fiber motions in half period are shown in Fig.6. In this example, both fibers translate with the bulk flow in the z direction, because two fiber centroids are initially located at $y_c^A = y_c^B = 0.1$ mm, where the bulk fluid has a translation velocity with $U_z = \dot{\gamma} y = 0.1$ mm/s.

In terms of cylindrical fibers, we use the equivalent aspect ratio (r_e^*) to describe fiber motions, i.e., $r_e^* = 6$, and it will have the same rotation as that of an ellipsoidal fiber with $r_e = 6$. From [6], the cylinder's geometric aspect ratio is $r_e = 7.715$, i.e., $a = 0.386$ mm and $b = 0.05$ mm, where a is the length of cylinder, and b is the diameter of bottom surface. The initial configuration of two cylindrical fibers is shown in Fig.5(b), with $\phi_0^A = \phi_0^B = \psi_0^A = \psi_0^B = 0$, $\theta_0^A = \theta_0^B = 90°$, $x_c^A = x_c^B = 0$, $y_c^A = y_c^B = 0.1$ mm, $z_c^A = -2$ mm, $z_c^B = 2$ mm and $D = 4$ mm. So $\zeta = a/D = 0.0964 \ll 1$. The comparison between our data and Jeffery's single fiber solution is tabulated in Table 2 for both ellipsoidal and cylindrical fibers. We find that the motions of two far-away cylindrical fibers

still follows Jeffery's solution with the equivalent aspect ratio used to quantify fiber motions.

TABLE 1. Parameters to simulate two far-away ellipsoids

Properties	Parameters
fiber size (ellipsoidal fibers)	long axis: $a = 0.3$ mm
	short axis: $b = c = 0.05$ mm
	geometric aspect ratio: $r_e = \frac{a}{b} = 6$
fluid domain	$H = 12$ mm, so $\varepsilon = 0.025$
initial orientation (cf.Fig.5(a))	$\phi_0^A = \phi_0^B = \psi_0^A = \psi_0^B = 0$, $\theta_0^A = \theta_0^B = 90°$
initial position (cf.Fig.5(a))	$x_c^A = x_c^B = 0, y_c^A = y_c^B = 0.1$ mm, $z_c^A = -2$ mm, $z_c^B = 2$ mm, so $D = 4$ mm, and $\zeta = 0.075 \ll 1$
properties of bulk fluid	viscosity: $\mu = 100$ pa·s
	Shear flow: $U_z = \dot{\gamma} y$, where $\dot{\gamma} = 1$ s^{-1}

6

TABLE 2. Deviation of our data from Jeffery's single fiber solution

Average of relative errors	for two ellipsoids ($r_e = 6$)	for two cylinders ($r_e = 7.715, r_e^* = 6$)
ϕ^A (degree)	0.04%	0.2%
ϕ^B (degree)	0.1%	0.08%
y_c^A (mm)	0.7%	0.2%
y_c^B (mm)	0.7%	0.1%
z_c^A (mm)	0.6%	0.2%
z_c^B (mm)	0.2%	0.02%

Therefore, when fibers are far away from each other, i.e. $\zeta \ll 1$, the hydrodynamic interactions are trivial, which do not have obvious effects on fiber motions, which can still be predicted by Jeffery's theory.

4.1.2 Fibers are close to each other When ζ is comparable with or greater than 1, the effect of hydrodynamic interactions on fiber motions can be observed obviously. In this section, we give three examples to model the hydrodynamic interactions between two close fibers, and study the corresponding effects on fiber motions as two fibers move closer to each other.

Example 1: Two horizontal cylindrical fibers with $\zeta = 0.95$

The configuration of two cylindrical fibers are shown in Fig.5(b). In this example, we use the same fluid domain and bulk fluid as those in Table 1. Only the initial configurations of fibers are different, which are tabulated in Table 3.

**TABLE 3**. Parameters to simulate two close cylinders

Properties	Parameters
fiber size (cylindrical fibers)	length: $a = 0.386$ mm
	diameter: $b = 0.05$ mm
	$r_e = \frac{a}{b} = 7.715, r_e^* = 6$ (see ref. [6])
initial orientation (cf.Fig.5(b))	$\phi_0^A = \phi_0^B = \theta_0^A = \theta_0^B = 90°$
	$\psi_0^A = \psi_0^B = 0$
initial position (cf.Fig.5(b))	$x_c^A = x_c^B = 0, y_c^A = y_c^B = 0.1$ mm,
	$z_c^A = -0.2029$ mm, $z_c^B = 0.2029$ mm,
	so $D = 0.4058$ mm, and $\zeta = 0.95$

The motion of a single cylindrical fiber with the equivalent aspect ratio $r_e^* = 6$ would have the same periodic tumbling motion as that of an ellipsoidal fiber with geometric aspect ratio $r_e = 6$ (see ref. [6] and section 4.1.1). With the presence of another cylindrical fiber in close proximity, the fiber motion will be slowed down, with the time period of fiber motions compared with that predicted by Jeffery's theory in Table 4, from which we find that the short-range hydrodynamic interactions slow down fiber motions. Therefore, we posit that the slow motion observed in refs. [2] and [3] could result from fiber-fiber interactions in semi-dilute suspensions.

TABLE 4. Results of time periods of fiber rotations

Scenarios	Two close cylinders	A single cylinder	Relative error
Time period	43.2 s	38.75 s	11.5%

The fiber motions and local velocity distribution around fibers in the y direction are shown in Fig.7.
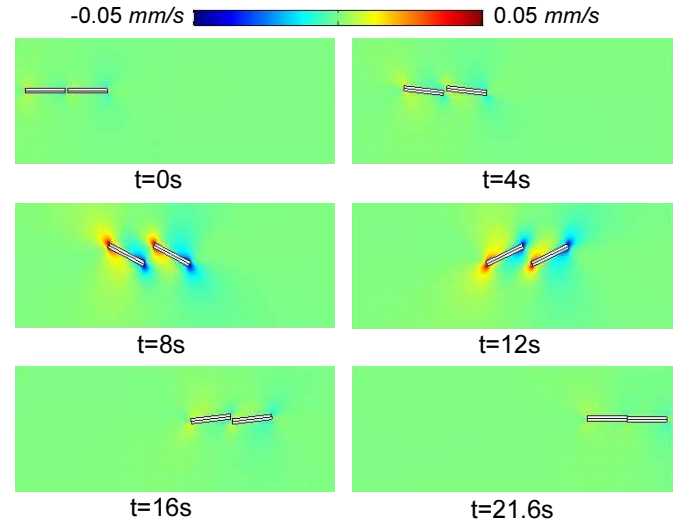
FIGURE 7. Fiber motions and velocity distribution in the y direction

Example 2: Two horizontal cylindrical fibers with $\zeta = 0.97$

This example is similar to example 1, but with a closer distance between fiber centroids. In this example, we still use two horizontal cylindrical fibers, with $z_c^A = -0.198$ mm, $z_c^B = 0.198$ mm, so $\zeta = 0.97$, which is closer to 1. All other parameters are the same as those in example 1.

The plot of fiber positions and orientations in half period is shown in Fig.8, from which we find that the short-range
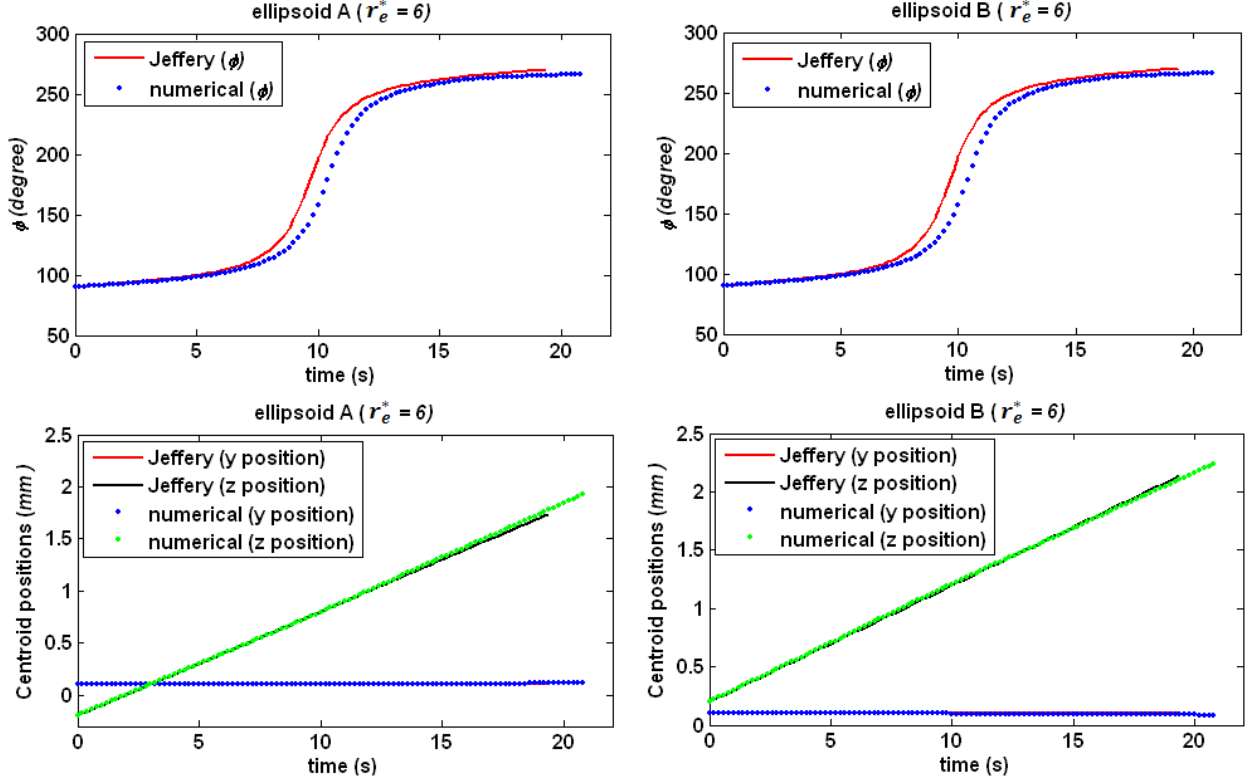
FIGURE 8. Fiber positions and orientations in half period: two adjacent cylindrical fibers ($\zeta = 0.97 \approx 1$)

hydrodynamic interactions move the fibers off Jeffery's trajectory, and slow down fiber motions. In this example, two cylindrical fibers has a physical contact at $t = 20.8\ s$. After the collision, multiple fibers will become a floc, and move together, which is beyond the scope of this paper. By comparing example 1 and 2, we find that as fibers move closer to each other, inter-fiber hydrodynamic interactions become stronger, and the deviation from Jeffery's trajectory gets more obvious.

Example 3: Two vertical ellipsoidal fibers with $\zeta = 1.5$

When ζ is greater than 1, i.e., the distance between fiber centroids is less than fiber size, the hydrodynamic interactions becomes stronger, and the possible physical/mechanical contacts happen more frequently. The initial configuration of two ellipsoidal fibers ($r_e = 6$) can be seen in Fig.5(a), with the initial configurations: $\phi_0^A = \phi_0^B = \psi_0^A = \psi_0^B = 0, \theta_0^A = \theta_0^B = 90°$ and $x_c^A = x_c^B = y_c^A = y_c^B = 0, z_c^A = -0.1\ mm, z_c^B = 0.1\ mm$. Therefore, $D = 0.2\ mm$, and $\zeta = 1.5 > 1$.

The local velocity distribution around fibers in the y direction and the motions of two ellipsoidal fibers are simulated in Fig.9 as a function of time. The plot of fiber positions and orientations in half period is shown in Fig.10. We see that fiber motions apparently deviate from Jeffery's single fiber solution, and fibers do not translate with the undisturbed simple shear flow

evaluated at fiber centorids. Instead, fibers have up-and-down motions and the collision happens at $t = 13.6\ s$ in this example.

4.2 Effect of bounded wall

The fiber motion with the presence of a bounded wall is simulated and the slow motion is observed with large ε, i.e., the size of fluid domain is comparable with fiber dimension (cf.
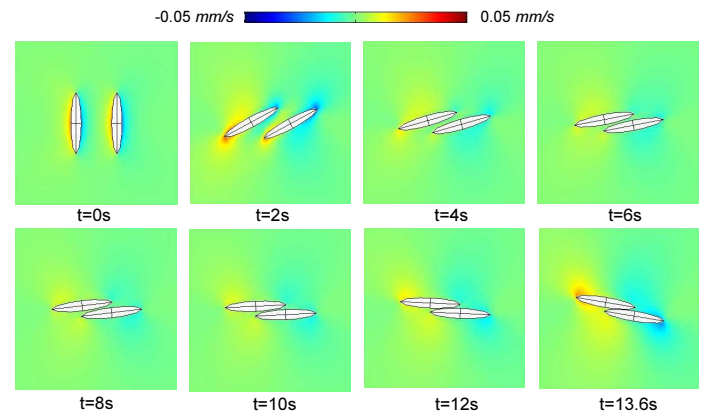

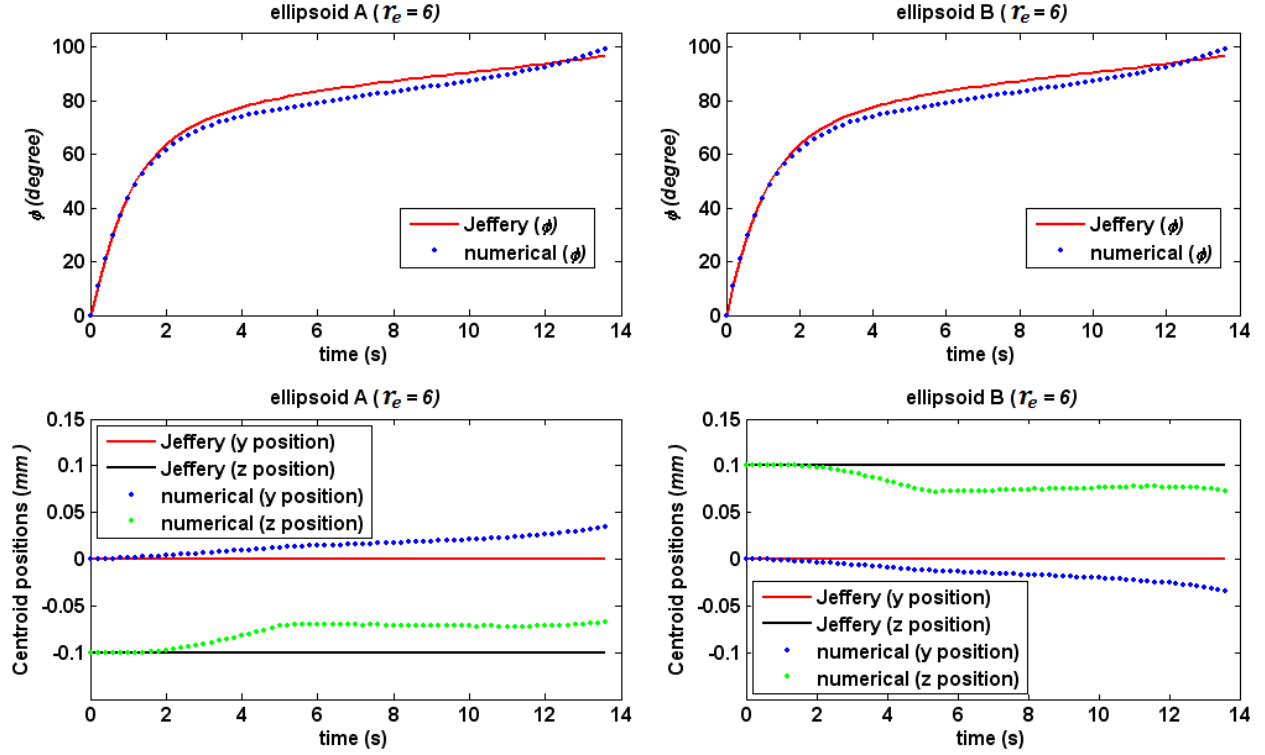**FIGURE 9.** Fiber motions and velocity distribution in y direction

8

FIGURE 10. Fiber positions and orientations in half period: two closer ellipsoidal fibers ($\zeta = 1.5 > 1$)

Fig.3). In this section, we model fiber motions in a bounded wall with different sizes of fluid domain, and the simulation parameters are set up in Table 5.

TABLE 5. Parameters of a single ellipsoidal fiber in a bounded wall

Properties	Parameters
fiber size (ellipsoidal fiber)	$a = 0.3\ mm,\ b = c = 0.05\ mm$ $r_e = \frac{a}{b} = 6$
fluid domain	$H = 0.5\ mm,\ 1\ mm,\ 6\ mm$ or $12\ mm$ $\varepsilon = 0.6,\ 0.3,\ 0.05$ or 0.025
initial configuration	$\phi_0 = 0,\ \theta_0 = 90°,\ \psi_0 = 0$ $x_c = 0,\ y_c = 0,\ z_c = 0$
properties of bulk fluid	viscosity: $\mu = 100\ pa \cdot s$, $U_z = \dot{\gamma}\, y$, where $\dot{\gamma} = 1\ s^{-1}$

The fiber orientations and time periods according to different fluid sizes are shown in Fig.11, from which we can see that when $\varepsilon \leq 0.025$, the true percent relative error of time period compared with that obtained from Jeffery's solution is below 0.08%. And the time periods of fiber rotations increase as ε increases, i.e., the dimension of fluid domain become closer to fiber size. The slow fiber motion observed in [2] and [3] could also be attributed to the effect of a bounded wall (cavity).
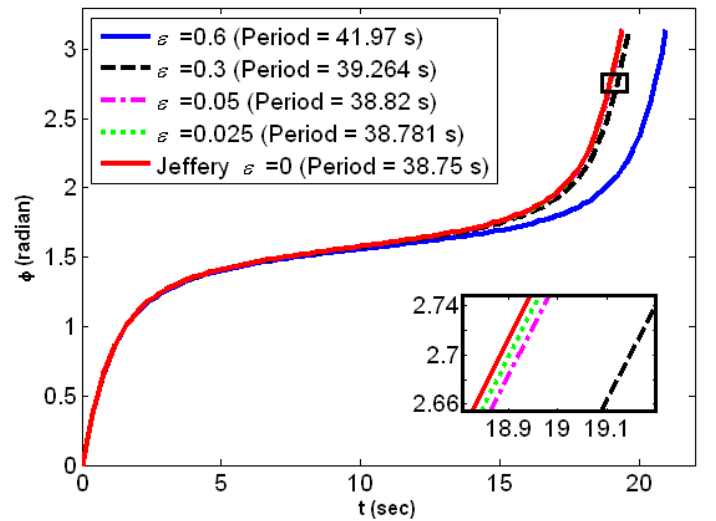

FIGURE 11. Effect of bounded wall on fiber orientations

9

5 CONCLUSION AND FUTURE WORK

In this paper, a methodology, which combines a finite element method, a Newton-Raphson method and a Runge-Kutta method, is proposed to solve the motion of multiple suspended fibers, including ellipsoidal and cylindrical fibers within a viscous fluid. The hydrodynamic interactions between fibers and the effect of a bounded wall are studied. Both these two issues are about the disturbance effects of the presence of other objects (fibers or a bounded wall) on fiber motions. We find that the hydrodynamic interactions only take effect when two fibers are close to each other, which could slow down fiber motions. Additionally, the wall effect is found to retard fiber motion in our simulations.

For the future work, this work will be extended to study concentrated fiber suspensions, i.e., the volume fraction of fibers is so high that physical/mechanical contacts dominate.

REFERENCES

[1] Jeffery, G. B, 1922. "The motion of ellipsoidal particles immersed in a viscous fluid". *Proc. Roy. Soc. London. Series A, Containing Papers of a Mathematical and Physical Character, 102*(715), pp. 161–179.

[2] Taylor, G. I., 1923. "The motion of ellipsoidal particles in a viscous fluid". *Proc. Roy. Soc. London. Series A, Containing Papers of a Mathematical and Physical Character, 103*(720), pp. 58–61.

[3] Wang, J., O'Gara, J. F., and Tucker III, C. L., 2008. "An objective model for slow orientation kinetics in concentrated fiber suspensions: Theory and rheological evidence". *Journal of Rheology, 52*(5), pp. 1179–1200.

[4] Stover, C. A., Koch, D. L., and Cohen, C., 1992. "Observations of fibre orientation in simple shear flow of semi-dilute suspensions". *Journal of Fluid Mechanics, 238*, pp. 277–296.

[5] Bretherton, F. P., 1962. "The motion of rigid particles in a shear flow at low reynolds number". *Journal of Fluid Mechanics, 14*(2), pp. 284–304.

[6] Zhang, D., Smith, D. E., Jack, D. A., and Montgomery-Smith, S. "Numerical evaluation of single fiber motion for short-fiber-reinforced composite materials processing". *ASME Transactions Journal of Manufacturing and Science Engineering*. Accepted for publication.

[7] Advani, S. G., and Tucker III, C. L., 1987. "The use of tensors to describe and predict fiber orientation in short fiber composites". *Journal of Rheology, 31*(8), pp. 751–784.

[8] Junk, M., and Illner, R., 2007. "A new derivation of jeffery's equation". *Journal of Mathematical Fluid Mechanics, 9*(4), pp. 445–288.

[9] Batchelor, G. K., 1970. "The stress system in a suspension of force-free particles". *Journal of Fluid Mechanics, 41*, pp. 545–570.

[10] Dinh, S. M., and Armstrong, R. C., 1984. "Rheological equation of state for semi-concentrated fiber suspensions". *Journal of Rheology, 28*(3), pp. 207–227.

[11] Folgar, F., and Tucker III, C. L., 1984. "Orientation behavior of fibers in concentrated suspensions". *Journal of Reinforced Plastics and Composites, 3*(2), pp. 98–119.

[12] Cintra, J. S., and Tucker III, C. L., 1995. "Orthotropic closure approximations for flow-induced fiber orientation". *Journal of Rheology, 39*(6), pp. 1095–1122.

[13] Mackaplow, M. B., and Shaqfeh, S. G., 1996. "A numerical study of the rheological properties of suspensions of rigid, non-brownian fibres". *Journal of Fluid Mechanics, 329*, pp. 155–186.

[14] Rahnama, M., and Shaqfeh, S. G., 1995. "The effect of hydrodynamic interactions on the orientation distribution in a fiber suspension subject to simple shear flow". *Physics of Fluids, 7*(3), pp. 487–506.

[15] Yamane, Y., Kaneda, Y., and Dio, M., 1994. "Numerical simulation of semi-dilute suspensions of rodlike particles in shear flow". *Journal of Non-Newtonian Fluid Mechanics, 54*, pp. 405–421.

[16] Fan, X. J., Phan-Thien, N., and Zheng, R., 1998. "A direct simulation of fibre suspensions". *Journal of Non-Newtonian Fluid Mechanics, 74*(1-3), pp. 113–135.

[17] Claeys, I. L., and Brady, J. F., 1993. "Suspensions of prolate spheroids in stokes flow. part 1. dynammics of a finite number of particles in an unbounded fluid". *Journal of Fluid Mechanics, 251*, pp. 411–442.

[18] Stover, C. A., and Cohen, C., 1990. "The motion of rodlike particles in the pressure-driven flow between two flat plates". *Rheologica Acta, 29*, pp. 192–203.

[19] Jayageeth, C., Sharma, V. I., and Singh, A., 2009. "Dynamic of short fiber suspensions in bounded shear flow". *International Journal of Multiphase Flow, 35*, pp. 261–269.

[20] Batchelor, G. K., 1967. *An Introduction to Fluid Dynamics*. Cambridge University Press.

[21] Durbin, P. A., and Medic, G., 2007. *Fluid Dynamics with a Computational Perspective*. Cambridge University Press.